Journal of Power Sources 285 (2015) 413–417

Contents lists available at ScienceDirect

Journal of Power Sources

journal homepage: www.elsevier.com/locate/jpowsour

Short communication

Enhancing the quality of the tomography of nanoporous materials for better understanding of polymer electrolyte fuel cell materials

Severin Vierrath [a, *], Firat Güder [b, 1], Andreas Menzel [b], Matthias Hagner [d], Roland Zengerle [a], Margit Zacharias [b], Simon Thiele [a, c]

[a] Laboratory for MEMS Applications, IMTEK – Department of Microsystems Engineering, University of Freiburg, Georges-Koehler-Allee 103, 79110 Freiburg, Germany
[b] Laboratory for Nanotechnology, IMTEK – Department of Microsystems Engineering, University of Freiburg, Georges-Koehler-Allee 103, 79110 Freiburg, Germany
[c] FIT, University of Freiburg, Stefan-Meier-Straße 21, 79104 Freiburg, Germany
[d] Department of Physics/Nanostructure Laboratory, University of Konstanz, Universitaetsstrasse 10, 78457 Konstanz, Germany

HIGHLIGHTS

- A 3D reconstruction of a PEFC catalyst layer is obtained by FIB-SEM tomography.
- Pores of the catalyst layer are filled with ZnO by atomic layer deposition.
- Filled pores yield high contrast images, enabling more accurate reconstruction.
- Diffusivities are compared for ALD-filled and non-filled reconstructions.
- The distribution of large Pt clusters in the catalyst layer is investigated.

GRAPHICAL ABSTRACT

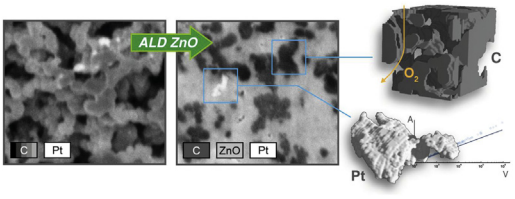

ARTICLE INFO

Article history:
Received 31 October 2014
Received in revised form
7 March 2015
Accepted 17 March 2015
Available online 21 March 2015

Keywords:
Polymer electrolyte fuel cell
Catalyst layer
FIB-SEM tomography
Atomic layer deposition
Diffusion
Segmentation

ABSTRACT

To investigate the nanostructure of polymer electrolyte fuel cell catalyst layers, focused ion beam – scanning electron microscopy (FIB-SEM) tomography is a common technique. However, as FIB-SEM tomography lacks of image contrast between the catalyst layer and its pores, state-of-the-art reconstruction methods by threshold cannot accurately distinguish between these two phases. We show that this inability leads to an underestimation of the porosity by a factor of nearly two, a reconstruction with channel-like artifacts and that these artifacts make it impossible to calculate reliable diffusivities. To overcome this problem, we fill the pores of the catalyst layer with ZnO via atomic layer deposition prior to tomography. By using atomic layer deposition, even smallest pores can be filled with ZnO, which exhibits a good contrast to the catalyst layer in SEM images. As a result, we present the porosity of the catalyst layer (65%) and its three-dimensional representation without typical reconstruction artifacts. Calculated O_2 diffusivities ($23.05–25.40 \times 10^{-7}$ m^2 s^{-1}) inside the catalyst layer are in good agreement with experimental values from the literature. Furthermore, filling with ZnO permits the identification of large Pt clusters inside the catalyst layer, which were estimated to reduce the catalyst surface area by 9%.

* Corresponding author.
E-mail addresses: severin.vierrath@imtek.de (S. Vierrath), simon.thiele@imtek.de (S. Thiele).
[1] Whitesides Research Group, Department of Chemistry and Chemical Biology, Harvard University, Cambridge, Massachusetts, USA.

http://dx.doi.org/10.1016/j.jpowsour.2015.03.110
0378-7753/

1. Introduction

Focused ion beam – scanning electron microscopy (FIB-SEM) tomography is a popular technique for the investigation of polymer electrolyte fuel cell (PEFC) catalyst layers due to its ability to resolve the nanoporosity [1–6]. In FIB-SEM tomography, a three-dimensional reconstruction of the porous material is obtained by successive FIB milling and SEM imaging. However, a major drawback of this method is the lack of image contrast between solid particles and the pore space of nanoporous materials such as the PEFC catalyst layer (Fig. 1b). Therefore, segmentation of the catalyst layer, i.e. accurate discrimination of these phases, is highly challenging [1,3,4,7]. However, correct segmentation is essential for the calculation of morphology and transport parameters, which can then be used to better understand the investigated material and develop improved materials.

Tomographic data sets of catalyst layers are commonly segmented by one of the following three approaches: manually [1–3], automated via threshold [4–6] or automated by applying a complex algorithm [8–10]. Pixel-wise segmentation by hand takes a very large amount of time and also depends on the very interpretation of the images by the operator. Hence, automatizing segmentation is inevitable to investigate larger areas, e.g. for better representativeness. However, the common automatization by threshold segmentation assigns pixels to a phase exclusively according to their gray value. It is thus not capable of distinguishing a solid particle from a pore with solid particles in the background, if they possess the same gray value. Only deep pores appear darker than the rest of the catalyst layer due to SEM shadowing effects and thus can be identified by their gray value. However, such discrimination is not possible for most of the catalyst layer. As a consequence, elaborate algorithms have been published, which compare successive SEM images to detect whether a pixel is affected by the FIB milling, and thus lies in the cutting plane and belongs to the solid phase [8–10]. However, due to insufficient accuracy, further research is necessary.

The most straightforward approach to circumvent the segmentation challenge is the use of a filling material in order to obtain a contrast between pores and solid particles that is high enough for accurate automated segmentation. Filling materials range from resins, epoxy [11] or silicone [12] to liquid metals [13]. However, finding a filling material that facilitates good discrimination between pores and solid materials is not trivial: Firstly, the wettability of the porous material for the filling material must be high so that all pores of the porous material can be filled. Otherwise small pores remain empty or pressure must be applied which, however, could potentially alter the porous material's structure. In addition, homogeneous filling of even nano-sized pores should be achieved without any change in the pore shape. It should be noted that the solidification of a resin could be accompanied by shrinking or outgassing. As the second major requirement, the filling material must have a good SEM material contrast to the porous material to be superior to other contrast mechanisms. As the SEM material contrast strongly depends on the atomic number [14], the filling material must consist of elements that are significantly heavier or lighter than the elements of the porous material. This is especially difficult when the sample of interest is a composite of several materials (e.g. the PEFC catalyst layers consisting of carbon, platinum and ionomer [15]). For these reasons, filling the catalyst layer with resins or Wood's metal normally fails to give a reliable structural representation of the pores in tomographic imaging [1].

In the approach presented here, we suggest atomic layer deposition (ALD) as a new pore filling method for fuel cell materials. ALD is capable of intruding into even the smallest pores [16]. Furthermore, an enormous variety of materials can be deposited using ALD [17]. This allows a filling material to be selected that exhibits a high contrast to the elements of the porous material at hand. Güder et al. successfully applied ALD for 3D visualization of nanopores in porous silicon produced by metal-assisted chemical etching and demonstrated the capabilities of this strategy [18]. In this study, we demonstrate the impact of ALD as a filling method for FIB-SEM tomography by filling the catalyst layer with ZnO using ALD. In the following, we first present the preparation of the catalyst layer for ALD infiltration, then the ZnO infiltration by ALD itself, the FIB-SEM tomography process and finally the post-processing to yield a 3D reconstruction. As a result, we are able to represent the diffusivities of the catalyst layer without any of the artifacts of state-of-the-art segmentation. We will then discuss new insights on the distribution of Pt inside the catalyst layer in detail.

2. Experimental

The investigated catalyst layer was the cathode side of a commercial Gore PRIMEA A510.1 M710.18 C510.4 PEMFC membrane electrode assembly. The Pt volume fraction (1.6 ± 0.2 vol%.) in the sample was calculated using the layer thickness (11.4 ± 0.8 μm) as determined by Thiele et al. [2], the Pt loading (0.4 mg cm^{-2}) according to the manufacturer, and the Pt density (21.45 g cm^{-3}).

2.1. Preparatory FIB milling

As ALD applies atoms layer-by-layer, homogeneously, onto the surface of the porous structure, clogging of the pores might block precursor diffusion into the inner sections, leaving unfilled cavities. Hence, to minimize the number of cavities, good accessibility for the precursors has to be ensured. In an initial ALD infiltration of the

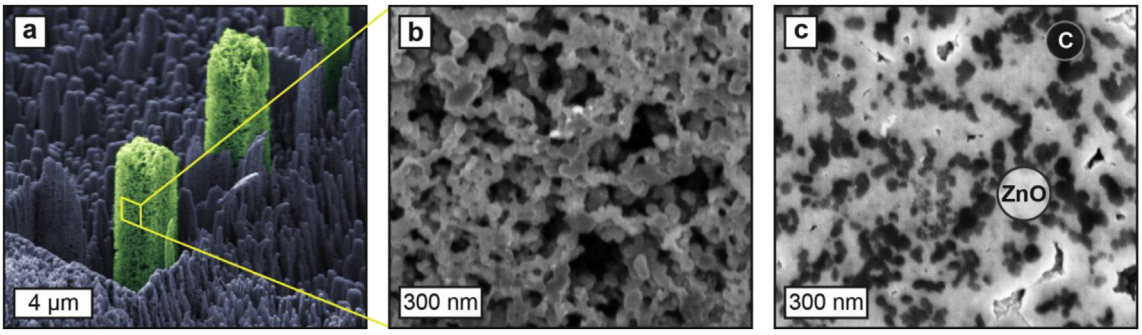

Fig. 1. PEFC catalyst layer a) FIB-milled towers for improved ALD precursor accessibility. b) FIB section of the catalyst layer before ALD filling. c) FIB section of the catalyst layer (dark) filled with ZnO by ALD (bright) taken in the middle of the tower. Contrast enhancement of pore space is clearly visible.

catalyst layer, we investigated the depth of infiltration and the effect on cavities. Although the catalyst layer's pore space was filled with ZnO down to a depth of approximately 1.5 μm, cavities, which later would complicate segmentation, remained in the former pore space. We hence decided that preparatory FIB milling prior to ALD was advisable. As the shape of a tower enables access to the inner sections, from at least four sides over the whole height, towers of 2 μm edge length were milled into the catalyst layer's structure with an FIB (Zeiss 'Neon 40EsB') prior to ALD infiltration (Fig. 1a). FIB currents ranged between 10 nA for rough cutting and 50 pA for polishing the towers' surface.

2.2. Atomic layer deposition of ZnO

After FIB milling the towers, the catalyst layer was coated with ZnO by allowing diethyl zinc and water to react in a cyclic manner (500 cycles) at 150 °C in a vertical-flow, hot-wall reactor (OpAL, manufactured by Oxford Instruments) as described in Ref. [18].

Fig. 1c shows a FIB section in the middle of the filled tower. As can be seen, the pores in the towers were filled entirely, leaving very few cavities. The measured ZnO film thickness was in good agreement with the predicted thickness of 80 nm (growth rate is 0.16 nm/cycle). No effect on the structure could be detected based on visual inspection by SEM, done before and after infiltration. On the contrary, filling the pore space with ZnO can be expected to reduce alteration of the structure caused by FIB milling: ZnO increases the stability of the porous structure and also its thermal conductivity. A better thermal conductivity, in turn, inhibits the formation of FIB-induced local hot spots, which is known to damage the ionomer phase of the catalyst layer [19].

2.3. FIB-SEM reconstruction and parameter calculation

With the towers filled with ZnO, part of a tower was reconstructed by FIB-SEM tomography with a Zeiss 'Neon 40EsB', comprising 170 FIB cuts and SEM images. Each FIB cut was conducted at 30 kV accelerating voltage and 5 pA beam current, with a cutting distance of 5.5 nm. SEM images were acquired at 5 kV with a pixel size of 1.861 nm using an in-lens detector. Image enhancement of the raw SEM image series was conducted with ImageJ [20]. Reconstruction followed the standard procedures of FIB-SEM tomography and was implemented in Matlab: image registration, geometrical corrections, cropping (1351 nm × 1351 nm x 940 nm) and segmentation. As illustrated in Fig. 1c, the gray values of ZnO differ markedly from those of the catalyst layer in the SEM images, facilitating very good discrimination between former pores and the solid phase. Segmentation, therefore, is trivial compared to the non-filled case. Remaining cavities, featuring similar gray values to the catalyst layer particles, can be identified with island filtering, as they are separated from the catalyst layer by a bright ZnO layer.

Bosanquet diffusivities were calculated in a cubic region of 940 nm edge length, using GeoDict as described in Ref. [21]. The surface area of the Pt clusters was estimated with VSG Avizo.

3. Results

The reconstructed catalyst layer featured a porosity of 65%, slightly greater than the 58% porosity of the same non-filled sample when determined by manual segmentation [2]. This could be explained by the general tendency of manual segmentation to overestimate the solid phase by assuming grains to be in the foreground rather than pore space with a grain in the background. Another possible explanation would be the lack of representativeness of either of the reconstructions. The segmentation of the non-filled sample via Otsu's threshold method yielded a porosity of 37% in contrast to the above values [22]. This very low porosity indicates the inability of this commonly used method to properly discriminate between pores and solid particles in the catalyst layer. The porosity, however, is very significant for the calculation of transport parameters. As can be seen here, Otsu's method results in a miscalculation by a factor of nearly two.

3.1. Diffusivity

To further demonstrate the accuracy of the ALD-filled reconstruction, we compared the three-dimensional representation and diffusivities to those of the non-filled reconstruction, shown in Fig. 2. To do this, we adjusted the threshold of the non-filled sample so that it approximately yields the same porosity as the ALD-infiltrated sample. As can be seen in Fig. 2a, the three-dimensional representation of the non-filled reconstruction shows a highly anisotropic structure featuring a predominant direction of the pores in the yz-plane of 54° with respect to the y-axis. The reason for these channel-like artifacts is obviously incorrect segmentation: Pore space is incorrectly identified to be solid phase, which is then shifted down according to the 54° perspective of the SEM with respect to the FIB cutting plane. The ALD-filled reconstruction, by contrast, exhibits an isotropic structure as one would expect from the isotropic catalyst layer (Fig. 2b).

To illustrate the impact of this error, O_2 diffusivities of both reconstructions were approximated with the Bosanquet formula [21]. Again, the diffusivity tensor of the non-filled reconstruction

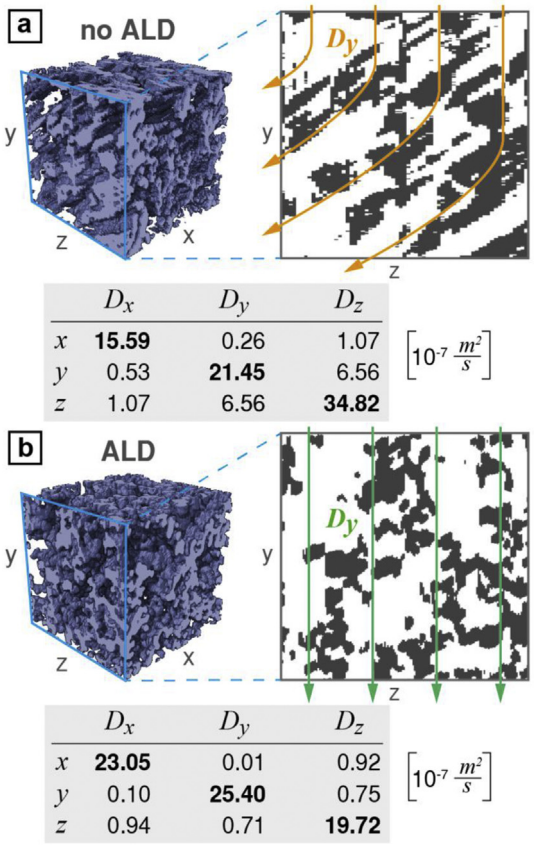

	D_x	D_y	D_z
x	**15.59**	0.26	1.07
y	0.53	**21.45**	6.56
z	1.07	6.56	**34.82**

$[10^{-7}\ m^2/s]$

	D_x	D_y	D_z
x	**23.05**	0.01	0.92
y	0.10	**25.40**	0.75
z	0.94	0.71	**19.72**

$[10^{-7}\ m^2/s]$

Fig. 2. Two reconstructions (three-dimensional representation, arbitrary yz plane as an example and Bosanquet diffusivities of O_2 in N_2) of the PEFC catalyst layer: (a) Non-filled reconstruction showing anisotropic structure and diffusion behavior due to incorrect segmentation. (b) ALD-filled reconstruction yields the correct isotropic structure and diffusion behavior.

features an incorrect anisotropy: The large discrepancy of all main diagonal entries ($15.59 \times 10^{-7} - 34.82 \times 10^{-7}$ m^2 s^{-1}) indicates anisotropy of diffusion inside the structure. The channel-like artifacts in the yz-plane increase diffusivities in y and z direction. Furthermore, large off-diagonal entries of y, z (6.56×10^{-7} m^2 s^{-1}) show the deviation which particles experience when diffusing in the y or z directions. By contrast, the x and y diffusivities of the ALD-filled reconstruction were calculated to be 23.05×10^{-7} m^2 s^{-1} and 25.40×10^{-7} m^2 s^{-1}, displaying only a minor difference. These values are in good agreement with the experimental results (24.10×10^{-7} m^2 s^{-1}) of Yu and Carter [23] for a similar catalyst layer with 68.1% porosity. Furthermore, no deviation of the particles occurs, as indicated by negligible off-diagonal entries. Please note that the diffusivity in the z direction (19.72×10^{-7} m^2 s^{-1} for the ALD-filled reconstruction) is inevitably lower in FIB-SEM tomography due to FIB cutting and consequential coarsening in the z direction [24]. However, for the z diffusivity of the non-filled reconstruction this decrease is superimposed by the strong increase due to channel-like artifacts. To summarize: ALD filling prior to segmentation gives a more realistic three-dimensional reconstruction and hereby enables more accurate calculation of diffusivities and presumably also other transport parameters. On the contrary, the strong discrepancy of the diffusivities of the non-filled reconstruction clearly shows that state-of-the-art automated threshold segmentation without prior ALD filling cannot be relied on.

3.2. Pt clusters

While filling the catalyst layer on the one hand ensures more accurate reconstruction of the catalyst layer's general morphology, it also aids the investigation of material distributions on the other: As filling the pores removes the 3D information from the SEM images, differences in the gray values of the solid particles, as observable in Fig. 1c, now depend solely on the material properties. In accordance with the dependence of brightness on the atomic number, lighter elements appear darker [14]. While most of the solid particles appear dark and thus mainly consist of carbon, some feature white dots, which represent Pt particles. The approximate size of these particles (less than 10 nm) corresponds to the typical particle size of maximum catalyst utilization [25]. However, the catalyst layer also contained some significantly larger Pt clusters as depicted in Fig. 3. 205 Pt clusters, several with a length greater than 100 nm, were found inside the reconstructed volume. It can therefore be assumed that approximately 12.7% of the Pt loading of 0.4 mg cm^{-2} is contained in clusters rather than being well dispersed, which would be unfavorable for a good catalyst layer. Furthermore, an estimation of the clusters' surface area reveals that these large clusters possess 74% less surface area than ideally dispersed 6 nm spheres. Fig. 3d shows the estimated surface area versus the volume for each cluster and for perfect spheres. As each cluster features a larger surface area than a sphere with the same volume, the reason for the overall loss of surface area lies in agglomeration. Thus 9% of the Pt required could be saved by preventing the formation of these agglomerates during manufacturing. Such clear details were not detected by any of the previously used methods, as conventional FIB-SEM tomography does not allow Pt to be identified unambiguously within the catalyst layer.

4. Conclusions

In summary, a fast and accurate method for three-dimensional reconstruction of fuel cell catalyst layer materials has been presented. This method combines ALD and FIB-SEM tomography to generate a stack of high-contrast SEM images that is well suited for automated computer-aided assessment. Filling with ZnO via ALD enhances the SEM contrast and reduces potential damage due to the FIB by increasing the porous material's stability and thermal conductivity. Based on FIB-SEM tomography of ALD-filled samples, three conclusions concerning the catalyst layer can be drawn from first data sets:

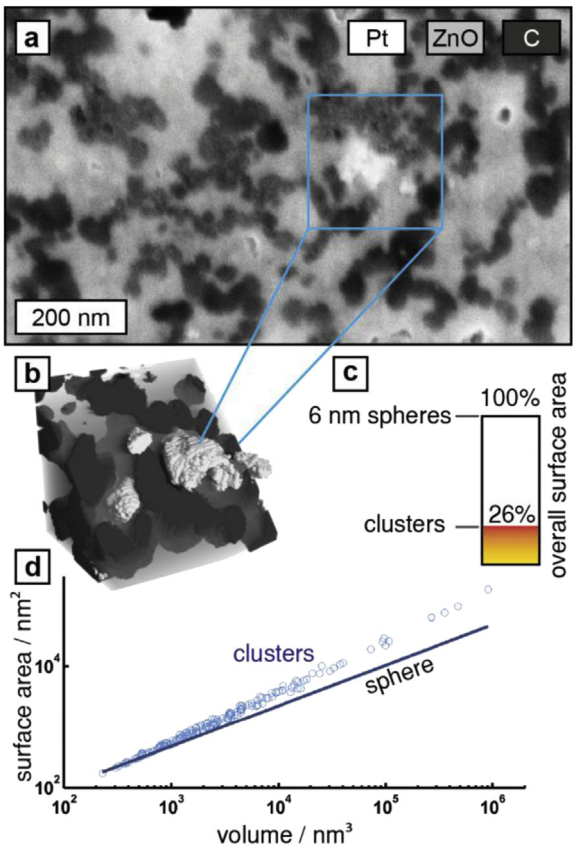

Fig. 3. Sample SEM image (a) and three-dimensional representation (b) of Pt clusters (very bright) in the catalyst layer (dark). Although all clusters have a better surface to volume ratio than spheres (d), their poor dispersion leads to a lower total surface area than 6 nm spheres (c).

- The catalyst layer has an isotropic structure with a porosity of approximately 65%.
- The x and y diffusivity values of O_2 within the catalyst layer have been approximated to be 23.05×10^{-7} m^2 s^{-1} and 25.40×10^{-7} m^2 s^{-1}, which is in good agreement with experimental results [23].
- Pt inside the catalyst layer is partly aggregated into large clusters, reducing the active surface area of the catalyst by 9%.

We demonstrated in this paper that state-of-the-art reconstructions by automated threshold segmentation are not able to yield correct porosity values and that they incorrectly predict highly anisotropic diffusion behavior. Furthermore, none of the published FIB-SEM studies were able to identify Pt clusters and their geometrical configuration. By contrast, our first experiments applying the new method presented here already demonstrate its superiority for obtaining a realistic 3D representation of the PEFC catalyst layer.

Considering the accuracy and the time saved by applying this new method, larger areas or multiple samples can be investigated in order to increase representativeness. This also allows, for

instance, studying the influence of process parameters of catalyst layer fabrication or studying morphology of the catalyst layer at multiple degradation states.

As an important next step we propose an extensive study of the ALD parameters, e.g. the diffusion time of the ALD precursors. Adjusting the ALD parameters could increase intrusion depth, which allows investigating thicker samples of catalyst layers over the whole height. For future reconstructions we recommend the use of fiducial marks to ensure accurate FIB cutting distances.

Acknowledgments

This work is part of the Gecko project (Grant No. 03SF0454C) and is funded by the German Federal Ministry of Education and Research (BMBF).

Appendix A. Supplementary data

Supplementary data related to this article can be found at http://dx.doi.org/10.1016/j.jpowsour.2015.03.110.

References

[1] H. Schulenburg, B. Schwanitz, N. Linse, G.G. Scherer, A. Wokaun, J. Krbanjevic, R. Grothausmann, I. Manke, J. Phys. Chem. C 115 (2011) 14236–14243.
[2] S. Thiele, T. Fürstenhaupt, D. Banham, T. Hutzenlaub, V. Birss, C. Ziegler, R. Zengerle, J. Power Sources 228 (2013) 185–192.
[3] J. Balach, F. Miguel, F. Soldera, D.F. Acevedo, F. Mücklich, C.A. Barbero, J. Microsc. 246 (2012) 274–278.
[4] K.J. Lange, H. Carlsson, I. Stewart, P.-C. Sui, R. Herring, N. Djilali, Electrochim. Acta 85 (2012) 322–331.
[5] R. Singh, A.R. Akhgar, P.C. Sui, K.J. Lange, N. Djilali, J. Electrochem. Soc. 161 (2014) F415.
[6] S. Zils, M. Timpel, T. Arlt, A. Wolz, I. Manke, C. Roth, Fuel Cells 10 (2010) 966–972.
[7] S. Thiele, R. Zengerle, C. Ziegler, Nano Res. 4 (2011) 849–860.
[8] P.S. Jørgensen, K.V. Hansen, R. Larsen, J.R. Bowen, Ultramicroscopy 110 (2010) 216–228.
[9] T. Prill, K. Schladitz, D. Jeulin, M. Faessel, C. Wieser, J. Microsc. 250 (2013) 77–87.
[10] M. Salzer, S. Thiele, R. Zengerle, V. Schmidt, Mater. Charact. 95 (2014) 36–43.
[11] J.R. Wilson, J.S. Cronin, S.A. Barnett, S.J. Harris, J. Power Sources 196 (2011) 3443–3447.
[12] M. Ender, J. Joos, T. Carraro, E. Ivers-Tiffée, Electrochem. Commun. 13 (2011) 166–168.
[13] L. Holzer, F. Indutnyi, P.H. Gasser, B. Munch, M. Wegmann, J. Microsc. 216 (2004) 84.
[14] L. Reimer, Scanning Electron Microscopy: Physics of Image Formation and Microanalysis, Springer, 1998.
[15] S. Litster, G. McLean, J. Power Sources 130 (2004) 61–76.
[16] M. Knez, A. Kadri, C. Wege, U. Gösele, H. Jeske, K. Nielsch, Nano Lett. 6 (2006) 1172–1177.
[17] M. Knez, K. Nielsch, L. Niinistö, Adv. Mater. 19 (2007) 3425–3438.
[18] F. Güder, Y. Yang, U.M. Küçükbayrak, M. Zacharias, ACS Nano 7 (2013) 1583–1590.
[19] V. Berejnov, D. Susac, J. Stumper, A.P. Hitchcock, ECS Trans. 50 (2013) 361–368.
[20] M.D. Abràmoff, P.J. Magalhães, S.J. Ram, Biophot. Int. 11 (2004) 36–43.
[21] J. Becker, C. Wieser, S. Fell, K. Steiner, Int. J. Heat Mass Transf. 54 (2011) 1360–1368.
[22] Nobuyuki Otsu, Trans. Syst. Man Cybern. 9 (1979) 62–66.
[23] Z. Yu, R.N. Carter, J. Power Sources 195 (2010) 1079–1084.
[24] M. Klingele, R. Zengerle, S. Thiele, J. Power Sources 275 (2015) 852–859.
[25] F.J. Perez-Alonso, D.N. McCarthy, A. Nierhoff, P. Hernandez-Fernandez, C. Strebel, Stephens, E.L. Ifan, J.H. Nielsen, I. Chorkendorff, Angew. Chem. Int. Ed. Engl. 51 (2012) 4641–4643.